PRELIMINARY RESULTS FOR $\bar{B}^0 \to D^+\ell^-\bar{\nu}$ DECAYS FROM CLEO

Roy A. Briere
Harvard University, Cambridge, MA 02138

Abstract

Two complementary analyses of $\bar{B}^0 \to D^+\ell^-\bar{\nu}$ decays at CLEO are presented. Consistent results for the branching ratios are obtained; these results are in agreement with expectations based on factorization and known hadronic branching ratios. In addition, the Isgur-Wise form-factor functions obtained from $\bar{B}^0 \to D^{*+}\ell^-\bar{\nu}$ and $\bar{B}^0 \to D^+\ell^-\bar{\nu}$ are compared.

1 Introduction

This talk will focus on two preliminary CLEO analyses of $\bar{B}^0 \to D^+\ell^-\bar{\nu}$ decays. This decay mode is interesting for several reasons. It is a poorly-measured part of the inclusive semileptonic rate. We can measure the $\bar{B}^0 \to D^+\ell^-\bar{\nu}$ form-factor and extract $|V_{cb}|$. Finally, this mode may be used in tests of the factorization hypothesis for hadronic decays.

2 Common Features of the Analyses

The CLEO detector has been described in detail elsewhere [1]. The most important features of the analyses be reviewed here.

CLEO takes data both at the $\Upsilon(4s)$ resonance, where $B\bar{B}$ pairs are produced, and at slightly lower energies to study off-resonance (continuum) $q\bar{q}$ production. About 1/3 of the data is taken at the lower energy. Both analyses use event-shape cuts to reduce continuum events and make use of off-resonance data to subtract the remaining background.

The D^+ is reconstructed in the $K^-\pi^+\pi^+$ channel. Kaon and pion candidates are required to have ionization energy loss in the drift chamber consistent with expectations. Both e and μ channels are used. Electrons are identified by combining quantities such as shower shape, ionization loss, and the ratio of calorimeter energy to track momentum. Muons are identified by requiring penetration through 5 interaction lengths of material; they begin to be efficiently identified around 1.4 GeV/c.

3 Neutrino Reconstruction Analysis

The hermeticity of the CLEO detector can been exploited to provide a 'measurement' of a neutrino. One first measures the missing momentum and energy:

$$\vec{P}_{miss} = -\sum \vec{P}_i; \qquad E_{miss} = 2E_{\,beam} - \sum E_i \tag{1}$$

where the sums are over the momenta (energies) of all particles in the event. Care is taken to exclude false tracks and spurious calorimeter clusters from the sums.

Events with more than one lepton are rejected, since this implies the presence of more than one neutrino. In addition, the charges of all tracks in the event must balance within one unit in order to insure a good measurement. Typical resolutions for reconstructible events are 260 MeV (110 MeV/c) for E_{miss} ($|\vec{P}_{miss}|$). We then take $\vec{P}_\nu = \vec{P}_{miss}$ and $E_\nu = |\vec{P}_{miss}|$; we use $|\vec{P}_{miss}|$ since the resolution is superior to E_{miss}.

When extra particles are missing from a signal event, reconstruction usually fails. The effect of this on efficiency is modeled with the Monte Carlo; it is largely a matter of unobserved K_L's, and these are simply related to the easily measured K_S rates. However, background events

Table 1: Systematic errors on $\mathcal{B}(\bar{B}^0 \to D^+\ell^-\bar{\nu})$ from neutrino reconstruction. The first two columns list the systematic errors considered; the last two columns are a breakdown of various contributions to the 'neutrino detection' error, which is rounded up to 15% before use.

Source	Fractional Error (%)		Fractional Error (%)
Neutrino detection	15.0	Breakdown of neut. det. error	
Semi-correlated backgrounds	5.6	Track finding	12
Particle ID	5.0	Track smearing	4.5
Lepton veto	4.5	Fake tracks	4
Lepton fakes	2.5	Fake clusters	3
$D^*\ell\nu$ branching fractions	2.2	Cluster finding	3
Lepton finding	2.0	K_L^0 content	2
Luminosity	2.0	Secondary ℓ content	1.5
D^+ sideband subtraction	1.5	K_L^0 energy	1
$B \to D^{**}/D\pi\,\ell\nu$	1.2	Cluster smear	0.5
Total	17.9	Total	14.3
$\mathcal{B}(D^+ \to K^-\pi^+\pi^+)$	6.6		

with extra missing particles may end up in the signal region. These can be removed effectively by requiring that $M^2_{miss} \equiv E^2_{miss} - |\vec{P}_{miss}|^2$ is consistent with zero. The M^2_{miss} resolution is observed to vary as $2E_{miss}\,\sigma_{E_{miss}}$; the cut employed is -0.45 GeV $< M^2_{miss}/2E_{miss} < 0.30$ GeV.

Given the four-vector of the neutrino, standard techniques for full reconstruction of B decays can be used.[3)] The key variables are the energy difference ΔE and the 'beam-constrained' B mass, M_B.

$$\Delta E = E_{\,beam} - \sum E_i \tag{2}$$

$$M_B = [E^{\,2}_{\,beam} - |\sum \vec{P}_i|^2]^{1/2} \tag{3}$$

where the sums are now over all particles, including the neutrino, belonging to the candidate B decay. Use of E_{beam} improves the mass resolution by a factor of about 10. Cuts of -500 Mev $< \Delta E <$ 100 Mev and 5.2650 GeV $< M_B <$ 5.2875 are imposed. The ΔE cut is asymmetric since feed-down background from D^{*+} and D^{**} decays is characterized by positive ΔE, due to the extra pions from the resonance decays. Decays are described by a form-factor depending on q^2, defined as:

$$q^2 = (E_B - E_D)^2 - |\vec{P}_B - \vec{P}_D|^2 \tag{4}$$

which can be easily evaluated given the inferred neutrino.

This analysis examined 2.63×10^6 $B\bar{B}$ pairs. Electrons were required to have a momentum of at least 0.8 GeV/c;

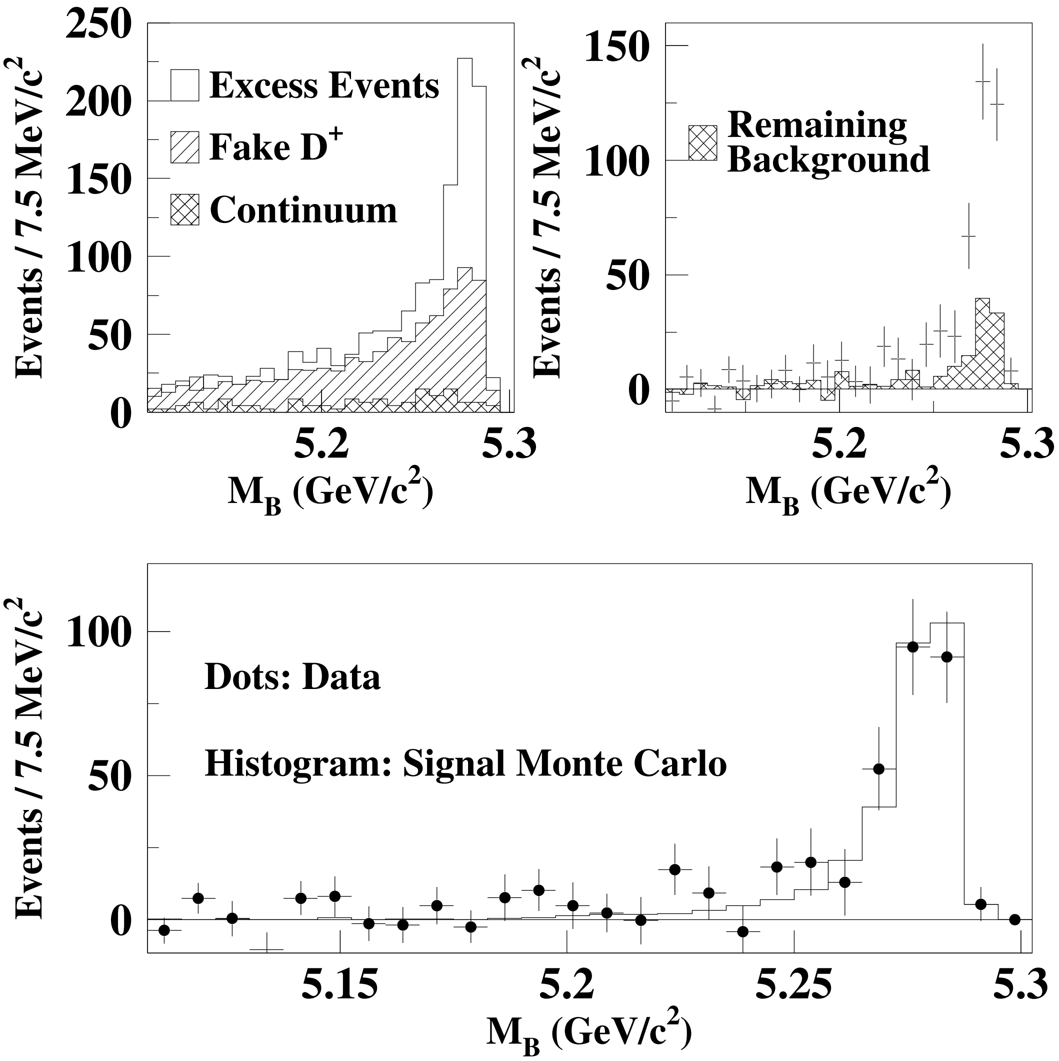

Figure 1: The B mass spectrum at various stages of the neutrino-reconstruction analysis. The first plot shows the continuum and D^+ sideband subtractions and the initial data sample. The next plot shows the excess after these first corrections, along with the final subtractions (mostly real D^+ and peaking $K\pi\pi$). The bottom plot compares the measured signal to a Monte Carlo simulation.

There are many backgrounds to consider. Continuum background is subtracted using the off-resonance data. The contribution of fake D^+ is removed with a side-band subtraction in the D^+ mass. These backgrounds are illustrated in the first plot of Fig. 1. A large part of the remaining background is due to real $D+$ from $D^{*+} \to D^+\pi^0$ decays; many of these are vetoed by attempting to reconstruct the D^{*+} and requiring that $|M_{D^*} - M_D| > 3$ MeV. Remaining backgrounds of real D^+ from D^*+ and D^{**} are modeled with the Monte Carlo. We also subtract backgrounds that peak in the $K\pi\pi$ mass distribution near the D^+ (avoiding the sideband subtraction), and contributions of fake leptons. The combined effect of these is also illustrated in Fig. 1. The final shape agrees quite well with our Monte-Carlo simulation. The M_B cut retains the highest three data points.

Many detailed systematic studies have been performed. The results are summarized in Table 1.

4 Missing-Mass Analysis

A more standard analysis technique for semileptonic decays has also been used. 2.15×10^6 $B\bar{B}$ pairs were examined. Leptons were required to have a momentum of at least 1.4 GeV/c.

In this 'missing-mass' technique, one assumes that the D^+ and lepton are from a real $\bar{B}^0 \to D^+\ell^-\bar{\nu}$ decay. One then constructs the missing mass implied for the neutrino:

$$\begin{aligned} MM^2 &= (E_B - (E_D + E_l))^2 - |\vec{P}_B - (\vec{P}_D + \vec{P}_l)|^2 \qquad (5) \\ &\approx (E_{beam} - (E_D + E_l))^2 - |\vec{P}_D + \vec{P}_l|^2 \qquad (6) \end{aligned}$$

We have used $\vec{P}_B \approx 0$ to obtain the second line.

One cannot evaluate q^2 exactly in the absence of neutrino information. If one ignores $\vec{P}_B$, one finds:

$$q^2 \approx E_{beam}^2 - 2E_{beam}E_D + M_D^2 \qquad (7)$$

In fact, we do better by using our knowledge of $|\vec{P}_B|$ (obtained from E_{beam}) to obtain minimum and maximum allowed values of q^2. The average of these values provides an improved estimate of the true q^2.

The analysis proceeds by fitting the D^+ yield for lepton-tagged events in 360 bins distributed in MM^2 and q^2. The resulting MM^2 distributions in each 2 GeV$^2/c^2$ bin are then background-subtracted and fit to extract the final signal.

The major background is real D^+ from $\bar{B}^0 \to D^+X\ell^-\bar{\nu}$ decays. There are two major components giving D^+X. The first is $\bar{B}^0 \to D^{*+}\ell^-\bar{\nu}$ with $D^{*+} \to D^+\pi^0$. This component can be measured directly, by reconstructing the D^{*+}, and then appropriately scaled and subtracted. The remaining D^+X are from D^{**} and non-resonant $D^+\pi$ states. These are harder to subtract; instead the shapes of their MM^2 distributions are determined from Monte Carlo. They are then fit concurrently with Monte-Carlo MM^2 shape for the $\bar{B}^0 \to D^+\ell^-\bar{\nu}$ signal to extract results.

The systematic errors considered are summarized in Table 2.

5 Comparison of Methods

The average efficiency of the neutrino-reconstruction analysis is 2.6%, while for the missing-mass analysis, it is 13%. The smaller efficiency is largely due to cuts required to ensure that the neutrino-reconstruction can be done cleanly. However, since the B mass is not used as an input with this method, one gets the much better background rejection of full reconstruction.

Table 2: Systematic errors on $\mathcal{B}(\bar{B}^0 \to D^+\ell^-\bar{\nu})$ for the missing-mass analysis.

Source	Fractional Error (%)	Source	Fractional Error (%)
Tracking efficiency	6.0	D^+ mass bkg. shape	4
D^{*+}scale factor	2.5	D^{*+} sideband subt.	1.4
K/π ID	2	Lepton ID	2
D^+ width	2	uncorrelated bkg.	2
fake lepton bkg.	1	MM^2 width	1.5
$D^+Xl^-\overline{\nu}$ model	< 2	$\mathcal{B}(D^+ \to K^-\pi^+\pi^+)$	6.6
		Total	11.3

In a clean mode, such as $\bar{B}^0 \to D^{*+}\ell^-\bar{\nu}$, the missing-mass technique does rather well, and the greater acceptance and simplicity are desirable. Such an analysis was used to measure $|V_{cb}|$.[2] The background rejection of the neutrino-reconstruction technique, however, was crucial in the first observation of exclusive $b \to u$ decays [4]. We have also used the neutrino technique to measure $B^- \to D^0\ell^-\bar{\nu}$.[5] This mode has a much larger 'feed-down' background from D^* decays, since these preferentially decay to D^0, rather than D^+.

6 Results

The results of the two analyses are summarized in Table 3. The statistical errors are somewhat independent; a large portion of these errors is from the background subtraction, which is very different in the two analyses. The first analysis also includes lower-energy electrons. Much of systematic error on the branching ratio is in shared.

The form-factor is defined as:

$$d\Gamma/dq^2 = G_F^2 |V_{cb}|^2 \, P_D^3 \, |f(q^2)|^2 \, / \, 24\pi^3 \tag{8}$$

We parameterize $f(q^2)$ as:

$$|V_{cb}f(q^2)| = |V_{cb}f(0)| \, e^{\alpha q^2} \tag{9}$$

and we report values for the intercept and exponential slope. The fractional errors on the intercept are essentially half those for the branching ratio.

7 Factorization

The semileptonic decay $\bar{B}^0 \to D^+\ell^-\bar{\nu}$ is very similar to the hadronic decay $B \to D^+h^-$ ($h = \pi \mathrm{or} \rho$). In the limit that the hadronizing W^- does not interact with the D, one may factorize the matrix element for the latter decay and obtain:

Table 3: Results.

Quantity	Missing-mass	Neutrino reconstruction
$\mathcal{B}(\bar{B}^0 \to D^+\ell^-\bar{\nu})$	$(1.75 \pm 0.25 \pm 0.21) \times 10^{-2}$	$(1.89 \pm 0.22 \pm 0.36) \times 10^{-2}$
$\lvert V_{cb} f(0)\rvert$	$(2.6 \pm 0.3 \pm 0.2) \times 10^{-2}$	$(2.49 \pm 0.24 \pm 0.22) \times 10^{-2}$
α (GeV^{-2})	$(3.1 \pm 2.3) \times 10^{-2}$	$(4.23 \pm 2.46 \pm 0.86) \times 10^{-2}$

$$\frac{\mathcal{B}(\overline{B^0} \to D^+ h^-)}{d\mathcal{B}/dq^2(\overline{B^0} \to D^+\ell^-\overline{\nu})|_{q^2=m_\pi^2}} = 6\pi^2 c^2 f_h^2 |V_{ud}|^2, \tag{10}$$

where f_h is the decay constant of the h^- meson, and c is a 'fudge' factor'; $c = 1$ in the naive factorization picture.

An evaluation of c using the data of the missing-mass analysis and previous CLEO measurements[3)] is given in Table 4. The results are consistent with factorization.

Table 4: Experimental determination of c from the missing-mass analysis. The third error on the hadronic branching ratio comes from the $D^+ \to K^-\pi^+\pi^+$ branching ratio, and thus cancels when evaluating c.

h^-	$d\mathcal{B}/dq^2$[GeV^{-2}]	$\mathcal{B}(\overline{B^0} \to D^+h^-)$[%]	f_h [MeV]	c
π^-	$0.36 \pm 0.05 \pm 0.04$	$0.29 \pm 0.04 \pm 0.03 \pm 0.05$	131.7 ± 0.2	$0.91 \pm 0.09 \pm 0.06$
ρ^-	$0.34 \pm 0.05 \pm 0.04$	$0.81 \pm 0.11 \pm 0.12 \pm 0.13$	215 ± 4	$0.97 \pm 0.10 \pm 0.08$

8 HQET and Form Factors

Heavy quark effective theory (HQET) is useful in the description of semileptonic B decays. In the limit of infinite heavy-quark masses, a very simple description emerges and corrections for finite quark mass can be expressed as a power series in $1/M_Q$.

Extractions of $|V_{cb}|$ from the form-factor of $\bar{B}^0 \to D^{*+}\ell^-\bar{\nu}$ are attractive since there are no corrections of order $1/M_b$ at $q^2 = q^2_{max}$. This is not true for $\bar{B}^0 \to D^+\ell^-\bar{\nu}$, or at other q^2. The corrections can be calculated, however, and are fairly small. It is interesting to compare the *measured* form-factors for $\bar{B}^0 \to D^{*+}\ell^-\bar{\nu}$ and $\bar{B}^0 \to D^+\ell^-\bar{\nu}$ to see directly if the corrections are small.

Figure 2 shows the HQET form-factor $F(w)$, where $w - 1 = (q^2_{max} - q^2)/2M_B M_D$. We also show $F(w)$ as determined from $\bar{B}^0 \to D^{*+}\ell^-\bar{\nu}$ [2)] and note that the two results are quite similar.

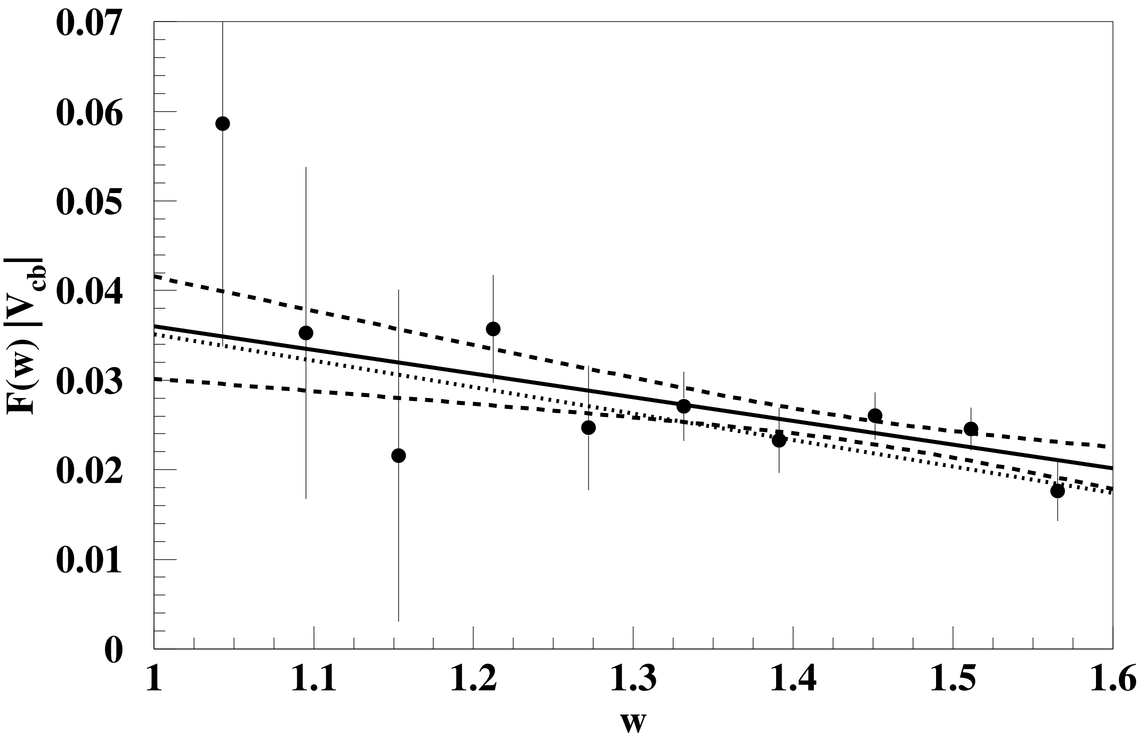

Figure 2: Isgur-Wise function from the neutrino-reconstruction analysis. The solid line is the measured from-factor from the neutrino-reconstruction analysis; the dashed lines show one std.-deviation errors. The dotted line shows the result obtained from a previous CLEO analysis of $\bar{B}^0 \to D^{*+}\ell^-\bar{\nu}$ [2].

9 Conclusion

We have presented new measurements of the branching ratio and form factor for $\bar{B}^0 \to D^+\ell^-\bar{\nu}$. We have shown naive factorization to work within our experimental errors, and have also shown the $\bar{B}^0 \to D^+\ell^-\bar{\nu}$ and $\bar{B}^0 \to D^{*+}\ell^-\bar{\nu}$ form-factors to be very similar, as expected from HQET. In the near future, results of the two methods will be combined, and results for $|V_{cb}|$ reported.

10 References

1. Y. Kubota *et al.* (CLEO Collaboration), Nucl. Instrum. Methods A **320**, 66 (1992).
2. B. Barish *et al.* (CLEO Collaboration), Phys. Rev. **D51**, 1014 (1995).
3. M.S. Alam *et al.* (CLEO Collaboration), Phys. Rev. **D50**, 43 (1994).
4. CLEO Collaboration, submitted to Phys. Rev. Lett.
5. Y. Kubota, *et al.* (CLEO Collaboration), CLEO CONF 95-10.